

1 **Replies to Technical corrections**

2
3 The article has been revised thoroughly by the authors. There were three minor reviews on this. The
4 authors have carefully attended all the points. The only concern at this stage is the technical
5 corrections. Kindly go through the text a few times and check for any errors, to enhance the quality
6 of the presentation of the science discussed herein. Here are some suggestions, but not complete.
7 Please make sure that you attend these suggestions before submitting the final version. I recommend
8 publication of the article after the technical corrections.

9 [First of all we wish to thank the reviewers and editors for going through the manuscript, offering](#)
10 [suggestions and appreciating the contents of the work. We have taken care of the comments/](#)
11 [suggestions made by the Editor.](#)

12
13 The line numbers follow the manuscript in the **Author response file**.

14 L 182: “Monsoon Inversion (MI) over Arabian Sea is one of the important characteristics ...”
15 [Reply : Corrected.](#)

16
17 L184: “five yearsof temperature and water vapour measurements obtained from”
18 [Reply: Profiles word is replaced by measurements.](#)

19
20 L210: level of temperature inversion?
21 [Reply: \(below 850 hPa\) is added.](#)

22
23 L215: more effect of what on MI?
24 [Reply: Sentence has been rephrased. The effect is on strength of MI.](#)

25
26 L217: spells of Monsoons?
27 [Reply: “spells” of active and break monsson refer to “periods”.](#)

28
29 L222: 1970-80s (no apostrophe)
30 [Reply: Corrected.](#)

31
32 L 240: as it moves
33 [Reply: “One” refers here to person. To avoid confusion, we have removed “as one moves” from the](#)
34 [text.](#)

35
36 L 242-243: opposite to the boundary of
37 [Reply: a portion of the senetence modified.](#)

38
39 L 246: over the Indian main land
40 [Reply: “the” added in the text.](#)

41
42 L 253: density? You mean frequency of the measurements...If yes, please state that.
43 [Reply: Density increase is not only just due to frequency of measurements, but also due to increased](#)
44 [resolution. We have replaced “density” with “number”.](#)

45 L 263-264: Please rephrase the sentence, as there are other ways / parameters that could also be used
46 for explaining subsidence and convection (in addition to winds).
47 [Reply: We have rephrased the sentence as: “For explaining the relative contribution of subsidence](#)
48 [and convection on MI, wind observations from ERA-interim reanalysis data have been used.”](#)

50 L 271, 280, 462, 604: There are a number of “viz” in this article, which sometimes breaks the flow of
51 the sentence. Kindly replace that word with appropriate synonym in other places.
52 Reply: Modified as:
53 L 271: viz retained
54 L 280 : “viz from” removed
55 L 462: viz replaced by “:”
56 L 480: viz replaced by “i.e.”
57 L 372: viz replaced by “like”
58
59 L 274-275: “...comparing the results”, not discrepancies, as the latter is what you infer from the
60 comparisons.
61 Reply: Modified as suggested.
62
63 L 283: “a short description of IS”?
64 Reply: “are” changed to “is”.
65
66 L 286-290: This sentence can be written at L 269, after “...2200 km”. It is a nadir looking
67 instrument and the vertical resolution can be coarse. The product may be available in interpolated
68 grids, but the resolution can be different. So please be sure about the resolution.
69 Reply: Sentence L286 -290 has been inserted at L296, after “...2200 km” as suggested. We have re-
70 checked the resolution.
71
72 L 308: “reference” is the appropriate word here.
73 Reply: “basis” is replaced by “reference”.
74
75 L 325: delete “in the present study”. It’s a waffle here.
76 Reply: Deleted.
77
78 L 327: “In this study, we use the data from surface to 600 hPa, which ...”
79 Reply: Text rephrased as “In this study, we use the data from surface to 600 hPa which have vertical
80 resolution of 30-20 hPa.”
81
82 L 328-329: Plz. write something like, “We use data from 2009 onwards to compare with other data
83 sets”. It is also good to state the last available year for the data (e.g. 2013).
84 Reply: Sentence modified as: “These data are available since 2003. We use data from 2009 - 2013 to
85 compare with other data sets.”
86
87 L 339: repetivity or frequency
88 Reply: We would like to retain “repetivity”. In satellite terminology this is a commonly used word.
89 L 343: “and moves to eastern ...”
90 Reply: “comes ” has been replaced by “moves”.
91
92 L 344: “MIs presence..”. This is what you have abbreviated earlier.
93 Reply: Modified from “MI’s” to “MIs”.
94
95 L 348: “and also in ...”
96 Reply: “of” is replaced by “in”.
97
98 L 349: “the temperature difference”
99 Reply: “the” word incorporated.

100
101 L 350: “so is a positive quantity.... ” and “between 6 and 7” or “ranging from 6 to 7”. Please write
102 either of this.
103 Reply: Suggestion incorporated “+” sign has to be retained to avoid confusion.
104
105 L 357-358; Please rephrase the sentence. You have measurements from the FGGE experiment and
106 you have derived or observed the MI features from those measurements.
107 Reply: sentence rephrased as : “Extensive AS MI features were observed from in-situ measurements
108 during FGGE-MONEX 1979 experiment.”
109
110 L 358: Delete bracket part for T, as you have already used this earlier in the text.
111 Reply: Deleted.
112
113 L 365: You have not stated this in the abstract, if you are “redefining MI” here
114 Reply: “redefining MI” is replaced with ” in depth study of”.
115
116 L 386: “However, to provide a margin of error..”
117 Reply: Sentence modified as : “However, to provide margin of error, we have still considered $\Delta T \leq$
118 $+2$ K as criterion of inversion region.”
119
120 L 393: “70%, as shown in Fig....”
121 Reply: Text is modified with “as shown in”.
122
123 L 404: “... bad profiles and are discarded.”
124 Reply: This sentence added after L404 as “Such bad profiles are discarded.”
125
126 L 419: passes or overpasses?
127 Reply: “passes” word is replaced by “overpasses”
128
129 L 422: “used only a section of these data sets”
130 Reply: Sentence rephrased as “For some studies (e.g. for Fig 2, 4, 5, etc), we have used only a
131 section of these data sets.”
132
133 L 435: “To show the efficiency and strength of currently available satellite measurements to
134 delineate features of MI over AS...”
135 Reply: Sentence rephrased as : “To show the efficiency and strength of currently available satellite
136 measurements to delineate features of MI over AS,”
137
138 L 455: “forms/appears around” instead of “start forming”
139 Reply: “start forming” is replaced by “appears”
140
141 L 458: “difference IS significant” or use just predominant
142 Reply: Suggestion incorporated.
143
144 L 466: “MI is found”
145 Reply: “seen” is replaced by “found”.
146
147 L 475-476: “.....coast, but the normalis restored towards the Indian Coast”

148 Reply: Sentence rephrased as : “The strength of MI can be noticed as $\sim + 2$ K near Arabia coast, but
149 the normal environmental lapse rate condition of $+ 6$ to $+ 7$ K/km is restored towards the Indian
150 coast.”
151
152 L 503: “data show”
153 Reply: modified “shows” to “show”.
154
155 L 504-505: Plz. write something like, “However, this feature is not observed or pronounced in the
156 ERA-interim data”
157 Reply: Sentence modified as: “However, this feature is not observed in the ERA-Interim data.”
158
159 L 516, “, with EAS values being lower” or similar wordings.
160 Reply: “with” word is added.
161
162 L 523-524: You may rephrase it, as it confuses “mesoscale monsoon features” with “activity of
163 monsoon”
164 Reply: The word ‘mesoscale’ is deleted.
165
166 L 527: “Gadgil and “
167 Reply: a space (gap) has been given between “Gadgiland” so it is now “Gadgil and”.
168
169 L 531: a comma before “provided” would make it more legible
170 Reply: Comma inserted.
171
172 L 539: Plz. Use another word for patchy such as discontinuous or incoherent
173 Reply: Discontinuous word is used.
174
175 L 540: You mean the amplitude of the Delta T is larger in the ERI? Plz. specify the period of
176 “monsoon break spells”
177 Reply: yes, the DT values are more in the ERA data. Monsoon break spell (30 July – 11 August
178 2009) is mentioned.
179
180 L 541: “ERA-interim (or ERI) data show”
181 Reply: Modified “shows” to “show”.
182
183 L 581: You may not call this as an artifact or a problem of the model, as the model is designed for
184 such a work. Please rephrase this.
185 Reply: The word artifact is removed. .
186
187 L 583-584: Please rephrase this sentence
188 Reply: Sentence rephrased as : “Among the satellite observations, IASI shows higher PO of MI days
189 than AIRS, except during 2012 over WAS.”
190
191 L594: “We have also analysed and compared the Delta T observed by..... The analysis suggests that
192 these two data sets cannot be merged/combined to study.....”.
193 Reply: Modified as suggested: “We have also analysed and compared the ΔT observed by IASI and
194 AIRS over WAS and EAS (figure not shown). The analysis suggests that these two data sets cannot
195 be merged to study”.
196
197 L660: monsoon break spells? Please state the time period too, to make it clear.

198 Reply: Spells means periods (time). Period is added eg (30 July – 11 August 2009).
199
200 L 662-663: “These features are also observed in the ERI data, but are restricted to some parts of
201 AS..... “
202 Reply: Sentence modified.
203
204 L 686: References: et al. should be replaced with all author names (e.g. L 679, 686, 688, etc.)
205 Reply: et al. replaced with all author names. Other references also corrected.
206
207 L 692: Das, P. K.
208 Reply: Corrected.
209
210 L 708: B. M.
211 Reply: Corrected.
212
213 L 713, 716: Plz. be consistent for “Curr. Sci.”
214 Reply: Now references are consistent.
215
216 L 755: “measured by radiosonde during MONEX experiment,”
217 Reply: Figure caption modified as suggestd.
218
219 L 761: “Figure 3. Base”
220 Reply: Gap is given between “3.Base” as “3. Base”.
221
222 L 763: The full stop must be after the sentence (after the bracket here).
223 Reply: Position of full stop corrected.
224
225 L 768, 771, 772: It is a bit confusing to use same as (a) and (b) and (c) and (d), etc.. Please write
226 detailed figure captions with minimum “same as”. Thank you.
227 Reply: Corrccted.
228
229 **Some more corrections are done by us as :**
230
231 L 194 - vis - a - vis (V made l/c)
232 L 195 - r small in refractivity
233 L 216 - have changed to 'has'
234 L 268 - 'present' brought before MI as 'presence of'
235 L 284 - 'is' included
236 L 298 - 'only' removed. Included 'our analysis'
237 L 316 - 316 - 'present study' brought from end to beginning
238 L321 – ‘pass’ replaced by ‘passes’
239 L 405 - 'more' removed
240 L 476 - 'with' added
241 L 479 - 'month' brought before as 'month of'
242 'region of' Somali removed.
243 L 481 - 'shown by' removed, reference put in bracket
244 L 488 - 's' included in show
245 L 494 - 'n' l/c in northern
246 L 497 - 'is' changed to 'are'
247 - ' for' removed, 'to' included

248 L 523-524 - 'largely , the' removed - comments of Editor to rewrite the sentence
249 L 525 - 'typically' removed
250 L 607 - 'have' replaces 'has'
251 L 617 - 'W' made l/c
252 L 642 - 'was' changed to 'were'
253
254

255

256

257

258

259

260

261

262 **Characteristics of Monsoon Inversions over Arabian Sea observed by Satellite Sounder and**

263 **Reanalysis data sets**

264

265 Sanjeev Dwivedi¹, M. S. Narayanan¹, M. Venkat Ratnam^{2*} and D. Narayana Rao¹

266

267 ¹Department of Physics, SRM University, Kattankulathur, Chennai - 603 203, India.

268 ²National Atmospheric Research Laboratory (NARL), Gadanki, Tirupati- 517 502, India.

269

270 * yratnam@narl.gov.in ; Phone: +91-8585-272123; Fax: +91-8585-272018

271

272

273

274 **Abstract**

275 Monsoon inversion~~s~~ (MIs) over Arabian Sea (AS) ~~is one of the are-an~~ important
276 characteristics associated with the monsoon activity over Indian region during summer monsoon
277 season. In the present study, we have used five years (2009 - 2013) data of temperature and water
278 vapor ~~profiles~~measurements obtained from satellite sounder instrument, Infrared Atmospheric
279 Sounding Interferometer (IASI) onboard MetOp satellite, besides ERA - Interim data, to study their
280 characteristics. The lower atmospheric data over the AS have been examined first to identify the
281 areas where monsoon inversions are predominant and occur with higher strength. Based on this
282 information, a detailed study has been made to investigate their characteristics separately in eastern
283 AS (EAS) and western AS (WAS) to examine their contrasting features. The initiation and
284 dissipation times of MI, their percentage occurrence, strength etc., has been examined using the huge
285 data base. The relation with monsoon activity (rainfall) over Indian region during normal and poor
286 monsoon years is also studied. WAS ΔT values are ~ 2 K less than those over the EAS, ΔT being
287 temperature difference between 950 and 850 hPa. A much larger contrast between WAS and EAS in
288 ΔT is noticed in ERA-Interim dataset ~~y~~is a ~~y~~is those observed by satellites. The possibility of
289 detecting MI from another parameter, ~~r~~Refractivity N, obtained directly from another satellite
290 constellation of GPS RO (COSMIC), has also been examined. MI detected from IASI and
291 Atmospheric InfraRed Sounder (AIRS) sounder onboard NOAA satellite have been compared to see
292 how far the two data sets can be combined to study the MI characteristics. We suggest MI could also
293 be included as one of the semi-permanent features of southwest monsoon along with the presently
294 accepted six parameters.

295

296 *Keywords:* Monsoon inversion, Arabian sea, lower atmospheric temperature, satellite sounders,
297 IASI, ERA

298

299

300 **1. Introduction**

301 The Monsoon Inversion (MI) is one of the criteria providing a stability condition over the
302 western Arabian Sea (AS), extending sometimes through to the west coast of India. The MI controls
303 the mid tropospheric moisture content during the different phases of the monsoon. This shallow layer
304 of low level inversion (below ~ 800 hPa) will act as a barrier in uplifting of the moisture, and could
305 act like a wave – guide for transport of water vapour to the mainland. The fluctuation of the rainfall
306 over the west coast of India is more closely related to changes in monsoon circulation over the AS
307 (Das, 2002). The AS is located at the north head of the Indian Ocean. During the monsoon season,
308 Indian rainfall is ~~fully~~ dependent on the physical processes occurring over AS like SST, Somali
309 Low Level Jet and ~~the near by it~~ advection of hot air from the Arabian desert, ~~is there which~~ These
310 is have profound putting more effect on strength of MI. Thus, MI has been known to be intimately
311 associated with the activity of the Indian southwest monsoon and ~~has~~ ve a close link with active and
312 break spells (Narayanan and Rao, 2004).

313 MIs were first detected in 1964 during International Indian Ocean Expedition (IIOE) from
314 ship radiosonde data by Colon (1964) and Ramage (1966). Subsequently from satellite derived
315 temperature and humidity data, this feature was detected by Narayanan and Rao (1981). They
316 detected MI despite the coarse vertical resolution (~ 2 km) of the TIROS – N satellite temperature
317 sounding instruments (Thomas, 1980) of 1970 – 80's compared to the vertical extent (about 1 to 1.5
318 km) of the phenomena itself. They used a simple differencing technique by finding the difference,
319 ΔT , of sea skin temperature and 1000 to 850 hPa mean layer temperature (MLT) from the satellite
320 sounding data. By adopting this differencing procedure, they assumed that most of the systematic
321 errors/limitations of retrieval methods and vertical resolution of satellite soundings may be getting
322 significantly minimized. Furthermore, the spatial and temporal nature of MIs is quite large compared
323 to normal boundary layer inversions observed over land and other oceans.

324 Using data of about 150 ship radiosonde and aircraft dropsonde profiles and concurrent
325 TIROS – N satellite sounder data of MONsoon EXperiment (MONEX) conducted in 1979, they
326 showed that regions with $\Delta T \leq 2$ K in satellite derived atmospheric temperatures are associated with
327 AS MI. Study of these MIs over the western AS was one of the three major objectives of MONEX /
328 FGGE -1979 (WMO, 1976). These are seen to be much stronger (temperature departures from
329 normal profiles in some cases being as high as ~ 6 K in the lower 1 - 2 km height region) in contrast
330 to the inversions observed over land or associated with trade wind inversions ($\sim 1 - 2$ K).

331 MIs are characterized by both a vertical temperature increase in the altitude region from 0.5
332 km (in some cases even from surface) to ~ 2 km and with a sharp fall in relative humidity (RH)
333 above this altitude region. Some of the observed features of MIs reported from the limited
334 observations to date (Colon, 1964; Ramage, 1966; Narayanan and Rao, 1981; 1989) are: (i) strength
335 decreases and base increases ~~as one moves from the~~ west to east AS, (ii) oscillation of its lateral
336 boundary from west to east with the activity of monsoon and (iii) associated oscillation of mid
337 tropospheric water vapor content from east to west, i.e. ~~in the opposite sense~~ to the boundary of
338 temperature inversion. The two primary causes proposed (Colon, 1964) for formation/maintenance
339 of monsoon inversion are: (a) hot air advection from Arabia (~ 700 hPa) riding over cool maritime air
340 (at levels below ~ 800 hPa) from south Indian Ocean and (b) subsidence over western AS associated
341 with monsoon convection over ~~the Indian~~ main land. This large scale subsidence had played a major
342 role in the maintenance of MI during the prolonged weak monsoon of 2002 (Narayanan et al., 2004).

343 However, not much attention was paid to the study of MI due to paucity of freely available
344 data over this region. The spatial density of TIROS – N satellite data available to the global
345 research community in 1979 was just a single temperature – humidity profile a day in a latitude –
346 longitude grid box of $2.5^\circ \times 2.5^\circ$ (Kidder et al., 1995). Narayanan and Rao (1981) had to adopt
347 temporally a pentad and spatially a $5^\circ \times 5^\circ$ average to detect statistically significant results from the
348 meager data available then. Since 2008, the ~~densitynumber~~ of temperature and humidity profiles

349 from polar orbiting satellites is nearly two orders of magnitude higher (about one vertical profile
350 every 50 x 50 km, twice each day and from two satellites) besides with a much better vertical and
351 spectral resolution. Thus, it has become possible now to study MI phenomena in greater detail.
352 However, no in-situ data after the 1979 experiment are available in this region.

353 In the present study, we have used the high resolution and better accuracy temperature and
354 humidity profiles data obtained from Infrared Atmospheric Sounding Interferometer (IASI) onboard
355 MetOp satellite. These data have higher vertical resolution, i.e., ~ 400 m below 700 hPa, which is
356 much better than those of TIROS – N of MONEX 1979 period. Further, ERA-Interim data have been
357 used to compare the MI features seen in them with those from the satellite data. For explaining the
358 relative contribution of subsidence and convection on MI, ~~where only~~ wind observations ~~are~~
359 ~~required, from~~ ERA-interim reanalysis data have been used. The temperature - humidity profile data
360 are also available from NOAA – Atmospheric InfraRed Sounder (AIRS) instrument since 2002, all
361 of which have also been analysed in the same way as the IASI data. However, we have not presented
362 those results here, because of some inconsistencies (i.e. sometimes ERA – interim data shows MI but
363 AIRS has different features like no presence of MI ~~present~~, profile to profile match between AIRS
364 and ERA-interim datasets are not seen i.e. inversion type changes or level of inversion changes)
365 observed between the IASI and AIRS data in studying the MI features. Thus, we have confined the
366 present study to data only from one instrument, viz., IASI, which had been reported to be performing
367 better (Smith et al., 2015). This is expected to also ensure that the results of temporal and spatial
368 gradients of ΔT presented here (featuring MI) will be mutually consistent – even if the absolute
369 values of temperature/humidity may be having some errors. We have, however, included one section
370 ~~describing the discrepancies between comparing~~ the results of these two instruments for studying the
371 MI features. We have also shown to a limited extent the potential of the GPS RO measured
372 ‘refractivity’ profiles in delineating inversion regions. For this we have also used the MONEX in-
373 situ temperature – humidity profiles of 1979.

374

375

376 2. Data

377 As mentioned earlier, data from a variety of instruments have been used in this study – viz
378 ~~from~~ IASI satellite instrument, ERA-Interim reanalysis data and, in-situ dropsondes/ radiosondes
379 data obtained during MONEX – 1979. Limited AIRS sounder data and GPS RO data have also been
380 presented for comparison purposes. A short description of each of these data ~~isare~~ given in the
381 following sub-sections and ~~is~~ also summarized in Table 1.

382 2.1. IASI observations

383 ~~The IASI instrument (Clerbaux et al., 2007; 2009) measures the profiles of temperature~~
384 ~~profiles in the troposphere and lower stratosphere with a high accuracy (~1K root mean square) at a~~
385 ~~vertical resolution of 1 km in the lower troposphere), as well as humidity profiles in the troposphere~~
386 ~~(10–15% accuracy with a 1–2 km vertical resolution) primarily for numerical weather prediction~~
387 ~~(Schlüssel et al., 2005).~~ IASI is a thermal infrared nadir-looking Fourier transform spectrometer
388 which measures the Earth’s surface and the atmospheric radiation over a spectral range of 645–2760
389 cm^{-1} with a 0.5 cm^{-1} spectral resolution. The IASI field of view is a matrix of $2^\circ \times 2^\circ$ circular pixels,
390 each with a diameter footprint of 12 km at nadir. It measures on an average at each location on the
391 Earth’s surface twice a day (at 09:30 and 21:30 hr local time), every 50 km at nadir, with an
392 excellent horizontal coverage due to its polar orbit and its capability to scan across track over a swath
393 width of 2200 km. The IASI instrument (Clerbaux et al., 2007; 2009) measures the profiles of
394 temperature profiles in the troposphere and lower stratosphere with a high accuracy (~1K root mean
395 square) at a vertical resolution of 1 km in the lower troposphere), as well as humidity profiles in the
396 troposphere (10–15% accuracy with a 1–2 km vertical resolution) primarily for numerical weather
397 prediction (Schlüssel et al., 2005). More details about retrieval and validation are presented in Kwon

398 et al. (2012). The support products, which we have used, are available at 100 pressure levels at 50 x
399 50 km horizontal grid spacing, but we restrict the data from surface to 600 hPa for our analysis only.

400 2.2. Dropsonde / Radiosonde measurements MONEX (1979)

401 For the in-situ ground truth comparisons over AS between the longitudes 55° -75°E we also
402 make use of the aircraft dropsondes and ship radiosonde observations obtained during MONEX
403 1979. MONEX was conducted during May - July 1979 and there were 416 radiosondes and 412
404 dropsondes measurements over AS. It may be noted that after the MONEX campaign in 1979, no
405 campaign has been organized to get in-situ data over western or central AS. During the Indian
406 ARMEX programme (2002), however, some in-situ data were available but only in the far eastern
407 AS (east of 70°) near the coast of India. Table 2 summarizes the comparison of in-situ observations
408 with satellite data of 1979 by Narayanan and Rao (1981). This information on ΔT criterion has been
409 used as the basis reference in the present study. In this regard it is worth to quote recent study by
410 Sanjeev Dwivedi et al. (2016) who has reported observations of temperature inversions during July -
411 August over Muscat and Salah (east Arabia coast) from concurrent radiosonde and IASI data.

412 2.3. ERA-Interim data

413 The European Centre for Medium Range Weather Forecasts (ECMWF)-Interim is one of
414 most advanced in operational use for diagnosing the global atmosphere with an accuracy that is less
415 than what is theoretically possible (Simmons and Hollingsworth, 2002; Simmons et al., 2007). The
416 selected variables are specific humidity along with the temperature on different pressure levels. The
417 atmospheric data are available at $0.125^\circ \times 0.125^\circ$ latitude and longitude grids on 37 pressure levels
418 from 1000 to 1 hPa; however, we have used for the present study, data of 14 pressure levels from
419 1000 to 600 hPa for the period of 2009 to 2013. for the present study. Vertical as well as horizontal
420 strength of MI have been examined from these data sets and compared with satellite observations.

421 2.4. AIRS observations

422 AIRS onboard the Earth Observing System (EOS) - Aqua satellite of NASA was launched in
423 2002. This is also a polar orbiting satellite which crosses the equatorial latitudes at 13:30 hr LT and
424 01:30 hr LT for the ascending and descending passes, respectively. The orbit period is 98.99 min,
425 and the orbit is sun synchronous with consecutive orbits separated by 2760 km at the equator. AIRS
426 has a field of view of 1.1° and provides a nominal spatial resolution of 13.5 km for IR channels and
427 approximately 2.3 km for visible/near-IR channels. AIRS data together with data from the Advanced
428 Microwave Sounder Unit (AMSU) (Lambrigtsen, 2003) are used ~~in the present study~~. We make use
429 of AIRS support data which have higher vertical resolution with 100 levels between 1100 and 0.016
430 hPa. ~~For the In present this~~ study, we ~~use restrict the~~ data ~~only~~ from surface to 600 hPa which have
431 vertical resolution of 30-20 hPa. ~~Though t~~ These data are available since 2003, ~~w~~ We ~~make~~ use data
432 from 2009 - ~~2013 only so as~~ to compare with other data sets.

433 2.5. COSMIC GPS RO

434 GPS RO technique is also a remote sounding satellite technique, and it uses the radio signals
435 received onboard a low Earth orbiting satellite from atmospheric limb sounding. The GPS RO
436 measurements have a vertical resolution ranging from 400 m to 1.4 km, which is much better than
437 that of any other satellite data (Kursinski et al., 1997). COSMIC has vertical resolution of ~ 100 m in
438 the lower troposphere for temperature. The COSMIC GPS RO was successfully launched in mid-
439 April 2006 (Anthes et al., 2008). Since 17 July 2006, COSMIC GPS RO provides accurate and high
440 vertical resolution profiles of atmospheric parameters that are almost uniformly distributed over the
441 globe. COSMIC provides a direct estimate of refractivity (from measurement of bending angle by
442 GPS technique) at very high vertical resolution, but have poor ~~repetivity. frequency repetivity.~~

443 3. Methodology and analysis procedure

444 As mentioned earlier, MI was first observed by Colon (1964) and Ramage (1966) over the
445 AS from ship upsonde profiles. They reported that MI lies between 900 and 800 hPa with strong
446 intensity over western AS (WAS) and weakens as its base rises and ~~move some~~ to eastern AS

447 (EAS). Following this study, Narayanan and Rao (1981) have shown MI's presence using the
448 temperature difference (ΔT) between the TIROS-N derived sea skin temperature and atmospheric
449 layer mean temperature (between 1000 hPa and 850 hPa).

450 Note that lapse rate (dT / dz) of atmosphere at the tropospheric altitudes is a negative
451 quantity. However, in this study (and also [in](#) Narayanan and Rao, 1981), we have considered ΔT
452 as [the](#) temperature difference between a lower level (higher temperature) and a higher level (lower
453 temperature), so is ~~normally~~ a positive quantity ~~of value between~~ $\sim + 6$ ~~and~~ $+ 7$ K. For inversion
454 regions, it is negative or a small positive quantity (i.e. less than $+ 2$ K).

455 After considering several limitations in the satellite data of that time, Narayanan and Rao
456 (1981) finally considered MI when the difference ΔT , between surface and layer mean temperature
457 (of 1000 to 850 hPa), is 2 K or less, which otherwise was greater than 3 K. Since then, several
458 improvements in the satellite instruments, retrieval techniques and data products have come up in
459 these three decades.

460 Extensive ~~in situ observations of~~ AS MI features were [observed from in-situ](#)
461 [measurements obtained](#) during FGGE-MONEX 1979 experiment. Fig. 1a shows a typical example of
462 MI observed in T (~~temperature~~) and RH (Relative Humidity) data obtained on 27 June 1979 at 0656
463 GMT at 20°N, 62°E from radiosonde. In this example MI starts from surface and temperature
464 departure is as high as ~ 10 K from a normal lapse rate profile at 900 hPa. The vertical extent of
465 inversion varies from 0.5 km to even more than 1 km. It is to be noted that AS MI are much stronger
466 and long lasting i.e. less diurnal variation than normal boundary layer and persist for many days
467 compared to those over land regions.

468 A detailed analysis is made in this study by considering several thousands of profiles
469 obtained from different satellite observations now available over AS for [redefining in depth study of](#)
470 MI. Since the MIs occur at low levels, first we tried with the earlier adopted criteria of Narayanan
471 and Rao (1981) i.e., by taking difference between sea surface (skin) temperature and 925 hPa level

472 (mean pressure level of 1000 - 850 hPa MLT of TIROS-N data of the 1980 time frame) temperature
473 and found those to be noisy for detecting MI. To avoid the surface emissivity effects in the retrieval
474 at / near surface (from the sounder instrument), we adopted the lower level in the present study as
475 950 hPa instead of sea surface / skin temperature. It was considered not appropriate to use SST/skin
476 temperature (though may be of higher accuracy) from a different source (~~like viz~~ imager onboard the
477 same satellite) for estimating ΔT . It was felt that this will not give the advantage of the differencing
478 procedure employed earlier to detect inversion (Narayanan and Rao, 1981). This level criterion (950
479 - 850 hPa) was arrived at after a detailed examination of ΔT at a few more level intervals (viz 1000 -
480 900 hPa, 1000 - 850 hPa, etc).

481 Thus, we have used:

$$482 \quad \Delta T = T(950 \text{ hPa}) - T(850 \text{ hPa}) \quad (1)$$

483 to delineate MI. However, the actual levels used were 958 hPa and 852 hPa at which the support data
484 are available from the NOAA website.

485 While considering the normal atmospheric lapse rate of + 6 to +7 K / km (average of 340
486 non-inversion cases obtained during MONEX, figure not shown), it is expected to observe a ΔT of
487 + 6 to +7 K between 950 and 850 hPa (~ 1 km height difference). Note that Narayanan and Rao
488 (1981) have identified inversion (non-inversion) region as $\Delta T \leq + 2 \text{ K}$ ($\Delta T > + 2 \text{ K}$) in TIROS - N
489 satellite data for a height range difference of ~ 0.75 km. For the present study (for 1 km height
490 difference) the same would translate to $\Delta T \sim + 2.7 \text{ K}$ for inversion delineation. However, ~~to be on~~
491 ~~the safe side and~~ to provide margin of error, we have still considered $\Delta T \leq +2 \text{ K}$ as criterion of
492 inversion region. The interval 2.0 K to 2.7 K may still be a grey region which could be interpreted as
493 inversion region on some occasions. The criterion of $\Delta T \geq + 4 \text{ K}$ as non - inversion regions has been
494 adopted. In the example shown in Fig. 1a, ΔT is (minus) - 1.3 K (note however, that the actual
495 inversion value is ~ - 5 K between surface and 900 hPa).

496 In general, a sudden drop in the water vapor just above the inversion is observed (e.g. RH
497 drop of ~ 70% [as shown](#) in Fig 1a). Since all the data sources mentioned in section 2 provide water
498 vapor information, we also have examined the changes happening in water vapor near/above the
499 inversion altitude. In general, inversion is identified in the temperature (water vapor) where it
500 increases (decreases sharply) instead of decreasing (decreasing gradually) with altitude. For
501 obtaining detailed characteristics of MIs over the Arabian sea, we have selected three 3° x 3° grid
502 boxes centered at latitude 18.5° N, and located at longitudes 60° E as WAS, 64° E as CAS (central
503 AS), 71° E as EAS (as shown in Fig.3).

504

505

506 **3.1. Quality checks for the profiles and volume of data**

507 Each temperature profile from the satellite data was interpolated from surface to 500 hPa (26
508 levels of support data) at 0.25 km intervals for our preliminary analysis. We have used the quality
509 flag 0 and 1 from the given data set which are corresponding to best and good. There were many
510 erroneous profiles which could be observed even from a cursory examination of the data. [Such bad](#)
511 [profiles are discarded](#). The temperatures at a few ~~more~~ levels were far wide of the normal profile.
512 To account for these types of profiles, we applied a quality check to filter out spurious data. All
513 profiles of July and August months of 2009 (poor monsoon year) and 2011 (normal monsoon year)
514 were sorted out in 3 x 3 boxes of WAS and EAS. For each month the mean and standard deviation
515 were obtained for each interpolated levels separately. Those profiles for which the data at any one
516 level was lying beyond + / - 2 sigma of the mean, were not considered for further analysis. From this
517 procedure we saw that nearly 25 – 30 % of profiles were getting filtered out.

518 Using these quality checked profiles, the procedure for selecting the right levels for
519 calculating ΔT was established. Thereafter, for all the other monsoon days of the five years, we have
520 computed ΔT for individual profiles by an automated procedure (without resorting to examining each

521 profile). They were grouped and their ΔT values averaged in $1^\circ \times 1^\circ$ bins over the whole AS region.
522 Diurnal variation of ΔT was examined for a few months of data. Once we made sure that this is not
523 discernible, the day and night data of a calendar day were merged in $1^\circ \times 1^\circ$ boxes.

524 For further analysis, the average ΔT values for the day (24 hr period) at $1^\circ \times 1^\circ$ grids have
525 been used. Due to averaging of ΔT of all the profiles in $1^\circ \times 1^\circ$ box and morning and evening
526 [overpasses](#) (~ 6 to 8 values of ΔT in 24 hours), the strength of MI may be getting somewhat reduced
527 (as MI occur at slightly different levels within a vertical range of 25 - 50 hPa, for different profiles in
528 the same $1^\circ \times 1^\circ$ box). For some studies (e.g. for Fig 2, 4, 5, etc), we have used only a [limited section](#)
529 [of these](#) -data ~~sets from this total data set~~. The total number of profiles considered for the five years
530 amount to nearly half a million, each for AIRS and IASI – considering that nearly 30 % profiles did
531 not pass through our quality check.

532 **4. Results and Discussions**

533 **4.1. Monsoon Inversions observed in satellite and ERA-Interim datasets**

534 Fig. 1a and 1b show MI observed on 27 June 1979 at 0730 GMT at 20°N , 60°E through
535 MONEX radiosonde and ERA – Interim data, respectively. The detailed comparison study between
536 TIROS – N satellite data of 1979 and concurrent in-situ MONEX radiosonde profiles for 1979
537 southwest monsoon carried out by Narayanan and Rao (1981) is summarized in Table 2. This was
538 the only occasion (1979) when in-situ data were available over AS to compare with satellite
539 soundings. Thus, comparison of current satellite observations is being done in this study with ERA-
540 Interim data. In this case, ERA – Interim data also catches the inversion but with a less rise in
541 temperature ($\sim 3 - 4$ K) and decrease in RH ($\sim 60\%$). To show [the efficiency and strength of](#)
542 [currently available satellite measurements to delineate features of MI](#) ~~how the present day satellites~~
543 [reveal MI over AS](#), typical profiles of temperature and RH obtained from collocated IASI and ERA-
544 Interim on 30 July 2009, 0530 GMT are plotted in Fig. 1c, and 1d, respectively. A clear MI in the
545 satellite profile and ERA-Interim can be noticed though with somewhat varying strengths and base of

546 inversion height. However, the top height of inversion is consistent. These are the first reported
547 results of MI features seen directly from the satellite observations over the AS which were shown
548 earlier by Narayanan and Rao (1981) in an indirect way by using ΔT indices. In general, in the
549 individual satellite profiles, we are able to see the MI strengths ranging from $\sim +2$ to -6 K (-8.8 K
550 being the actual temperature difference between 930 hPa and 850 hPa in Fig. 1c). These MI lie
551 mostly below 850 hPa level, but in rare occasions we could see them even up to 700 hPa over the
552 EAS – but of much weaker strength. The strength of MI is also seen to be decreasing from WAS to
553 EAS which will be discussed in detail in later sections.

554 Thus, in Fig. 1, we have seen examples of MI comparison between radiosonde and ERA
555 interim (1979) and between IASI and ERA-Interim (2009). There are some minor inconsistencies by
556 way of inversion heights in individual profiles of the three data sets. However, our objective here is
557 to examine the large scale characteristics of MI by considering average ΔT computed from individual
558 profiles in $1^\circ \times 1^\circ$ grids.

559 **4. 2. Contrasting behavior of MI between WAS and EAS**

560 As observed from Fig. 1, MI can lie between surface and ~ 2 km during Indian Summer
561 Monsoon (ISM) season (JJAS). Careful examination of time evolution of ΔT over the western
562 Arabian sea reveals that the MI ~~appears start forming~~ around first half of May and dissipate around
563 late September. Fig. 2 shows the evolution of the MI during two contrasting years (2009 a poor
564 monsoon year and 2011 a normal monsoon year). During the peak monsoon season of July – August,
565 the difference in ΔT between the two years ~~is are prominently noticed~~ significant. Also MI is more
566 frequently observed with higher strength during the peak monsoon months of July and August. To
567 investigate further their contrasting features in WAS and EAS, data only of July and August from
568 2009 to 2013 are presented.

569 In Fig. 3 we have summarized the three important characteristics of MI: ~~viz~~ their base
570 altitude, strength (as revealed by ΔT) and percentage occurrence during the complete season. For

571 brevity, the results of only July and August months, averaged for all the five years 2009 – 2013 are
572 shown in the figures. Fig. 3a and 3b show the spatial variation of base altitude of MI during July and
573 August, respectively. The contrasting feature of base altitude of occurrence of MI is foundseen
574 mainly north of 15° N from the selected three grid boxes. It increases from WAS (below 1 km) to
575 EAS (above 1.5 km) through CAS (1.0 -1.5 km).

576 As mentioned earlier, from very limited observations previous studies (Colon, 1964; Ramage,
577 1966; Narayanan and Rao, 2004) had suggested that strength and frequency of occurrence of the MI
578 days will be more over WAS than over EAS. To investigate this contrasting behavior of MI in detail
579 from satellite soundings, we examined the spatial variations of ΔT . Fig. 3c (July) and 3d (August)
580 shows the strength of MI increasing from EAS to the WAS and is prevalent mainly north of 15°N
581 latitude extending from 15°N to 25° N latitude and 55° E to 68° E longitude. The strength of MI can
582 be noticed as $\sim + 2$ K near Arabia coast, but the -and as we approach Indian coast, the normal
583 environmental lapse rate condition of $+ 6$ to $+ 7$ K/km are-is restored towards the Indian
584 coastencountered. From these figures a clear contrast in ΔT with a difference of around 2 K in the
585 southeast quadrant of AS between July and August is also noticed. In general, the AS is covered with
586 lapse rate of $+ 4$ K/km, which is the condition for taking the atmosphere towards stability during the
587 month of August-month. The region of Somali low level jet is the location of permanent region of MI
588 during the month of July. In the spatial distribution of monsoon low level jet shown by (Roja Raman
589 et al. (2011) reveals that the center of the core is seen around 13°N and 60°E and exists strong shear
590 between 850 hpa and 700 hpa. Strong surface winds of south-west monsoon produce an Ekman
591 transport perpendicular to the wind flow with strong upwelling in the region which in turn brings the
592 cool water from the deeper layers to surface. Simon et al. (2007) showed that WAS region is the
593 region of Somali upwelling, and also since the low level jet and surface wind are of the order of ~ 20
594 m/s, they produce sufficient cooling and the air above this region is still warmer when compared to
595 the upwelling area, producing strong inversion.

596 Fig. 3e and 3f show the spatial variation of percentage occurrence (PO) of MI during July
597 and August months. PO is calculated corresponding to $\Delta T \leq + 2$ K criteria. In general, it is observed
598 that WAS shows more number of MI cases (50 to 70%) compared to EAS (10 to 20%). ERA-Interim
599 data show only 30 to 50% cases of MI over WAS which will be dealt in detail in the following sub-
600 sections. The maximum PO during the four months of monsoon over the WAS are 40 % (June), 60
601 % (July), 50 % (August) and 30 % (September) (figure not shown). The areal extent of the maximum
602 PO is seen during July. During September, very small area of Northern AS is covered with ~ 50 %.
603 No inversion is seen in the EAS box during the June and September periods. Despite its low strength
604 (ΔT) PO show maximum occurrence of 60% in July. Since the PO and strength of MI over the CAS
605 ~~isare~~ in between the features of EAS and WAS, ~~for~~ further discussions pertain, only to WAS and
606 EAS boxes.

607 The PO of ΔT values in different ranges observed in IASI for the five monsoon seasons is
608 shown in Fig. 4. ΔT values range from -2 to + 6 K (0 to + 7 K) in WAS (EAS) with peak occurring
609 around + 1 to + 2 K (+3 to +4 K). There are only a few values of ΔT less than + 2 K in EAS. Similar
610 analysis is also made using ERA-Interim data and is shown in bottom panels of Fig. 4. ERA-Interim
611 data shows the contrast between WAS and EAS more clearly. In case of q at 700 hPa a difference of
612 about 2 g/kg can be noticed, with EAS having higher humidity values than WAS in IASI. However,
613 ~~this feature is not observed in the ERA-Interim data. does not show this distinction.~~

614 To further examine the contrasting behavior between EAS and WAS, time series of ΔT and
615 water vapour at 700 hPa is considered for different years. Daily mean variations of ΔT and specific
616 humidity, q, at 700 hPa in WAS and EAS during the monsoon season of the year 2012 observed by
617 IASI is shown in Fig. 5. Note that we have included results of all the days irrespective of whether MI
618 is present or not. Three point average smoothed curves are shown in the respective panels. In
619 general, it can be seen that WAS ΔT (q at 700 hPa) values are ~ + 2 K (1 - 2 g/kg) less than those
620 over EAS for the season as a whole (Fig. 5a and 5b). During all the years (2009 - 2013) of the

621 present study, IASI reveals (figure not shown) this feature. Similar analysis has been carried out
622 using ERA-Interim reanalysis data and is shown in Fig. 5c and 5d. A clear contrast between WAS
623 and EAS in ΔT can be noticed in ERA-Interim data. A mean difference of ~ 2 K (~ 1 g/kg) can be
624 noticed in ΔT (q at 700 hPa) between WAS and EAS, with EAS values being lower. A cyclic
625 behavior in ΔT variations with a period of ~ 20 -25 days in case of ERA-Interim is noticed but not
626 observed in the satellite measurements. There exists no significant diurnal variation in ΔT (figure not
627 shown). This was verified before averaging ΔT of all profiles (day and night) in the $1^\circ \times 1^\circ$ grids.
628 Due to inversion and stability, moisture is getting trapped at lower levels over WAS compared to
629 EAS as indicated in Fig. 5b and 5d observed from IASI and ERA-Interim, respectively.

630

631

632 **4.3. Relation between MI over AS and monsoon activity**

633 Past investigations (e.g. Gadgil and Joseph, 2003) showed that the **mesoscale** monsoon
634 features **largely** vary with **the** activity of the monsoon. In general during the active phase of the ISM,
635 **typically** there will be more precipitation over central India (18° - 28° N and 65° to 88° E). Similar
636 variations in precipitation during the monsoon season can also be expected on regional scales. Gadgil
637 and Joseph (2003), Kripalani et al. (2004), Rajeevan et al. (2006) have considered the daily rainfall
638 time series over central India during monsoon months along with the climate normal to delineate
639 'active' and 'break' periods over the Indian region. On the basis of this data, Rajeevan and Bhate
640 (2009) have defined active and break phases over central India by considering the days exceeding the
641 climate mean with +1 (-1) standardized anomaly as active (break) periods, provided it should persist
642 at least for 3 days (triad).

643 Fig. 6 shows the latitude - longitude cross section of ΔT and q at 700 hPa for active (14 - 17
644 July 2009) and break (30 July - 11 Aug. 2009) spells for the monsoon season of 2009 observed using
645 IASI and ERA-Interim data. Irrespective of the data source, ΔT and associated q at 700 hPa reveal

646 that a large part of WAS is covered with MI ($\Delta T \leq +2$ K and less moisture values) up to west of ~
647 68° E during the break spell as seen in Fig. 6a and 6e. In the north AS, MI reach as close as Gujarat
648 coast during break spells (especially in ERA-Interim data), but are restricted to WAS during active
649 spells. During the active spell, the inversion regions from ΔT maps are discontinuous west of
650 65° E in Fig. 6c. Also strengths of ΔT in WAS are more as observed by ERA-Interim than by IASI
651 during break spells (30 July – 11 August 2009). ERA-Interim shows (Fig. 6e and 6g) more smoothed
652 results and there is less change in area extent in this case. Specific humidity q at 700 hPa shows
653 clear result that during the break spell AS has less moisture and more during the active spell. One
654 can notice the feature of inversion from the figure where water vapor is being trapped in the lower
655 portion resulting in less moisture over WAS and more over the EAS. Thus, the q values also give a
656 good indication of the inversion feature.

657

658 **4.4. MI during normal and poor monsoon years**

659 It is well known that strong MI suppresses the vertical development of clouds; rain cannot
660 occur in such situations (Sathiyamoorthy et al., 2013). Using ARMEX-I (2002) data, Bhat (2006)
661 could notice strong and persistent inversions in the atmosphere over the AS and west coast of India.
662 This data proved very valuable as July 2002 rainfall was the lowest in the recorded history and the
663 data collected over the AS and on the west coast helped in understanding the conditions that
664 prevailed over the eastern AS during one of the worst monsoon years. The relation between MI and
665 central India rainfall is further investigated by separating the MI observed during normal (2010 -
666 2013) and poor monsoon (2009) years. Time variations of ΔT observed over WAS during two
667 contrasting years of 2009 and 2011 obtained from IASI measurements and ERA-Interim data are
668 shown in Fig. 7. It can be seen that good monsoon year 2011 has higher ΔT than poor monsoon year
669 2009 (Fig. 7a), and is the same for q i.e. higher value for the year 2011 (Fig. 7b). ΔT is observed to
670 be lower by about 2 K during the season as a whole in the poor monsoon year when compared to the

671 good monsoon year, suggesting the possibility of a variation of this parameter between normal and
672 poor monsoon years. This aspect is clear from the right panels where difference between 2011 and
673 2009 observed in ΔT (Fig. 7c) and q at 700 hPa (Fig. 7d) are shown. From this figure we can infer
674 that the year 2009 has less value of ΔT and less value for q suggesting stronger MI during poor
675 monsoon year. Note that during most of the time, the temperature in 2011 is higher (the difference
676 between 2011 and 2009 showing positive values) and less temperature lapse rate means more stable
677 layered atmosphere. In 2011, WAS temperature show higher values revealing less MI over AS when
678 compared to 2009. The decreasing trend in ΔT is discernible in difference plots for some particular
679 epochs. In general, ERA-Interim also show these features (Fig. 7e and 7f), but only to a moderate
680 extent. It may be noted that these inferences are based on the results of only one poor monsoon year
681 (2009).

682 683 **4.5. Inter-comparison of MI features with IASI, AIRS and ERA**

684 Inter-comparison of the gross features of PO of MI (with $\Delta T \leq 2$ K) in WAS and EAS
685 estimated for the five years of monsoon season by IASI, AIRS and ERA-Interim data are shown in
686 Fig. 8. In general, when we consider ΔT as a parameter to detect MI, clear contrasting feature
687 between WAS and EAS with higher PO in WAS can be noticed in all the data sources mentioned
688 above. PO in the IASI measurements ranges from 23% to 54%. Among these data sets, ERA-Interim
689 shows huge difference in the percentage occurrences between WAS and EAS, to the extent that not
690 even a single MI is seen in EAS in any year. Since the vertical resolution of the IASI temperature
691 profiles is better than AIRS, higher PO of MI in the WAS is noticed throughout when compared to
692 AIRS, except in the case of 2012. However, ERA-Interim being a combination of model and
693 observations, it is not able to pick up the MI in the EAS where the strength of inversion is also
694 weak. The ~~artifact of the~~ model appears to be smoothening the MI features of IASI when it is
695 assimilated in the ERA – Interim.

696 | ~~Among Coming to~~ the satellite observations, ~~during five years~~, IASI shows higher PO of MI
697 | ~~days~~ than AIRS, except ~~for~~during 2012 ~~over~~for WAS. A distinct contrast between WAS and EAS
698 | with higher PO in the former region can be noticed. When we consider EAS as a place to detect MI,
699 | AIRS observed always higher PO than IASI and almost nothing is noticed in ERA-Interim. Thus, we
700 | may infer that IASI is performing better than AIRS for detecting MI (as ERA is in better agreement
701 | with IASI rather than with AIRS). Note that large inter-annual variability in MI is observed and this
702 | is expected to reflect in the monsoonal activity over Indian region. It can also be seen that there is a
703 | steady decrease of PO of MI as observed by IASI from 2009 to 2013. No such feature is observed in
704 | AIRS – which shows more random behavior over the different years.

705 | We have ~~also made analysed the and compared~~ ~~scatter plot of the~~ ΔT observed by IASI and
706 | AIRS over WAS and EAS (figure not shown). The ~~analysis scatter does not~~ suggests that these two
707 | data sets ~~cannot~~ be ~~combined~~merged to study the small changes of ΔT in their intra-seasonal and
708 | inter-annual variations. This and the other differences related to q at 700 hPa constrained us not to
709 | combine the AIRS data with IASI data in the present study.

710 | **4.6. Monsoon Inversion derived from other parameters**

711 | Narayanan and Rao (1989) had also considered equivalent potential temperature (θ_e)
712 | differences to study MI. θ_e incorporates the effect of both temperature and humidity. However, the
713 | dynamic range of $\Delta\theta_e$ is no better than that of ΔT . Recall that the troposphere is statically stable on
714 | average, with a potential temperature gradient of 3.3 K/km (Wallace et. al., 2006). We make use of
715 | another index here ~~viz i.e.~~ atmospheric refractivity (N) for identifying MI. Similar to θ_e , Refractivity
716 | (N), is another atmospheric parameter which is a function of temperature and water vapor. It was
717 | shown that better information on boundary layer can be obtained from refractivity profiles than
718 | virtual potential temperature though both ~~have~~s temperature and water vapor information (Basha and
719 | Ratnam, 2009). Refractivity, N has a higher dynamic range and vertical variation as compared to
720 | temperature (~ 15 N units vis a vis 2 K). More advantage of using N for delineating MI will be

721 available, provided, it is measured directly, for example, using GPS Radio Occultation technique,
722 instead of computing it from temperature and water vapor obtained from the sounders or from
723 radiosonde. However, the spatio-temporal density of direct N observations is too sparse to get
724 meaningful statistics over equatorial regions.

725 We have computed refractivity N, from temperature and water vapor data of IASI (and
726 MONEX radiosonde data), given by the expression:

$$727 \quad N = 77.6 \left(\frac{P}{T} \right) + 3.73 \times 10^5 \left(\frac{e}{T^2} \right) \quad (2)$$

728 | [where](#) P is pressure, T temperature and e water vapor pressure.

729 Similar to ΔT we have defined an index ' ΔN ' as:

$$730 \quad \Delta N = N(950 \text{ hPa}) - N(850 \text{ hPa}) \quad (3)$$

731 Profile of N computed from the temperature and humidity profiles of dropsonde (Fig. 9a) of
732 MONEX time is shown in Fig. 9b. A drastic decrease in N (by 129 N units between 950 and 850
733 hPa) can be noticed near MI altitudes in this example. Thus, N can also be taken as a potential
734 parameter to delineate inversion and for studying spatial and temporal variations of MI.

735 In order to see the relation between ΔT and ΔN , we have estimated ΔN using all the MONEX
736 profiles obtained over AS. These include both inversion and non-inversion cases. There were 32
737 (346) profiles with inversion (non- inversion). Note that $\Delta T \leq + 2 \text{ K}$ and $\Delta T > + 4 \text{ K}$ are only
738 considered for obtaining above statistics and there exists 34 profiles in the transition zone (+ 2 to + 3
739 K). Scatter plot between ΔT and ΔN for all 411 in-situ profiles of MONEX over AS is shown in Fig.
740 9c. Correlation coefficients between the two parameters are found to be 0.56 with 15.7 as standard
741 deviation. Note that $\Delta T \leq + 2 \text{ K}$ (inversion region) corresponds to $\Delta N > 50 \text{ N units}$ which is shown
742 as blue line in Fig. 9c. We can infer that if ΔN is less than 50 N units it corresponds to non-inversion
743 region (ΔN more than 50 may be inversion or otherwise). ΔN is thus a supportive parameter to ΔT in

744 identifying inversion / non inversion. Because of its larger dynamic range, details of inversion have
745 been identified in the ΔT and ΔN maps (figure not shown).

746 It is well known that COSMIC satellites are able to provide N profiles directly. The spatial
747 and temporal sampling of COSMIC at any particular region are, however, very meager. The
748 comparison map of ΔN from IASI and ΔN from COSMIC combined for a long break spell from 30
749 July to 11 August 2009 has been studied. This long period accumulation of data was necessary to
750 have sufficient data points from COSMIC to cover the entire AS. One can see ΔN values above 50 N
751 units (inversion region) covering the entire Arabian sea corresponding to ΔT values being below 2 K
752 (shown by IASI, figure not shown). Over the AS region ΔN observed for all the five years of our
753 study ~~were~~was combined to produce the frequency distribution of ΔN over Western AS (5 – 25 °N,
754 56 – 65 °E, excluding land) and Eastern AS (5 – 25 °N, 66 – 75 °E, excluding land) and is shown in
755 Fig 10. Over WAS, 712 cases and over EAS 547 cases are showing $\Delta N > 50$ N units (which may be
756 supportive to inversion). A difference of about 10 N units can be noticed, with WAS having higher
757 ΔN values.

758 5. Summary and Conclusions

759 Low level MI characteristics, which usually occur below 700 hPa over the AS during
760 southwest monsoon months, have been identified directly from operational satellite temperature
761 retrievals. For the first time we have shown here cases of direct and unambiguous delineation of MI
762 from the satellite temperature and water vapor retrieval observations. We have used five years (2009-
763 2013) data of two different satellite sounder instruments (mainly from IASI and for inter comparison
764 AIRS) along with ERA-Interim reanalysis data to delineate the characteristics of MI over AS. Their
765 percentage occurrence, base height and strength have been studied. For supporting our findings, we
766 also compare with the campaign of MONEX 1979 in-situ measurements over AS. The main findings
767 obtained from the observational study are summarized in the following:

- 768 1. Percentage occurrences of MI over WAS (up to ~ 65°E) is ~ 60 – 70 % and are always higher
769 and stronger than over EAS. WAS ΔT values are ~ 2 K less than those over EAS.
- 770 2. MI is stronger during poor monsoon year (2009) and occurs on more occasions in WAS
771 during break spells [\(30 July – 11 August 2009\)](#). Whether this is true or not for all poor
772 monsoon years need to be checked with more years of data.
- 773 3. ~~These features are also observed in the ERA-Interim data, is also able to provide these~~
774 ~~features~~ but ~~are~~ restricted to some parts of AS -with more smoothed variability.
- 775 4. Inter-comparison of IASI and AIRS profiles from the view of study of inversion suggests the
776 differences do not warrant a mix of these two data sets for this study.
- 777 5. The refractivity data has only a supporting role to identify monsoon inversion regions.

778 Thus, MI seems to be a semi-permanent feature of Indian summer monsoon. It is suggested to
779 include this feature also in future monsoon diagnostic and forecast studies. The diagnostics from
780 ERA-Interim suggest the possibility of AS MI getting formed during mid May, primarily due to
781 subsidence mechanism and maintained later by the combined effects of advection and subsidence
782 which is the subject of our future study.

783

784 **Acknowledgments:** This work is a part of the INSAT – 3D project sponsored by the Indian Space
785 Research Organization (ISRO), for which we are thankful to Space Applications Centre,
786 Ahmadabad. We wish to thank C. M. Kishtawal, V. Sathiyamoorthy, S. Ghouse Basha, Jyotirmayee
787 and Ranjit Thapa for discussions and for help in data processing aspects and help in using HPCC.
788 The authors would like to thank ECMWF (<http://apps.ecmwf.int/datasets>) for providing data of ERA-
789 Interim, GESDISC(<http://mirador.gsfc.nasa.gov/>~~for AIRS~~)for AIRS, NOAA
790 (<http://www.nsof.class.noaa.gov/>for IASI) for IASI through ftp. We also thank IMD for providing
791 rainfall data over Indian land mass.

Formatted: Default Paragraph Font, Font: Calibri

792 **References**

793 [Anthes, R. A., Bernhardt, P. A., Chen, Y., Cucurull, L., Dymond, K. F., Ector, D., Healy, S. B., Ho, S. P.,](#)
794 [Hunt, D. C., and Kuo, Y. H.: Anthes, R. A., et al.:](#) The COSMIC/FORMOSAT-3 mission: Early
795 results, *Bul. Am. Meteorol. Soc.*, 89, [doi: 10.1175.1–21](#), 2008.

Formatted: Font: Times New Roman, No underline, Font color: Auto

796 Basha, G. and Ratnam, M. V.: Identification of atmospheric boundary layer height over a
797 tropical station using high-resolution radiosonde refractivity profiles: Comparison with GPS radio
798 occultation measurements, *J. Geophys. Res.*, 114, D16101, [doi:10.1029/2008JD011692](#), 2009.

Formatted: Font: Times New Roman, No underline, Font color: Auto

799 Bhat, G. S.: The Indian drought of 2002: a sub-seasonal phenomenon, *Q. J. Roy. Meteor. Soc.*, 32,
800 2583-2602, 2006.

801 [Clerbaux, C., Hadji-Lazaro, J., Turquety, S., George, M., Coheur, P. F., Hurtmans, D., Wespes, C., Herbin,](#)
802 [H., Blumstein, D., and Tourniers, B.: Clerbaux, C., et al.:](#) The IASI/MetOp mission: First observations
803 and highlights of its potential contribution to GMES, *COSPAR Inf. Bul.*, 19–24, 2007.

Formatted: Font: Times New Roman, No underline, Font color: Auto

804 [Clerbaux, C., Boynard, A., Clarisse, L., George, M., Hadji-Lazaro, J., Herbin, H., Hurtmans, D., Pommier,](#)
805 [M., Razavi, A., and Turquety, S.: Clerbaux, C., et al.:](#) Monitoring of atmospheric composition using
806 the thermal infrared IASI/MetOp sounder, *Atmos. Chem. Phys.*, 9, 6041–6054, 2009.

Formatted: Font: Times New Roman, No underline, Font color: Auto

807 Colon, J. A.: On interactions between the Southwest Monsoon Current and the Sea Surface over the
808 Arabian Sea, *Indian J. Met. Geophys.*, 15, 183 – 200, 1964.

809 Das, P. K.: The Monsoons, Nation Book Trust, New Delhi, India, ISBN 978-81-237-1123-2, 193,
810 2002.

811 [Dwivedi, S., Sathiyamoorthy, V., Narayanan, M. S., and Rao, D. N.: A Study on the Lower](#)
812 [Tropospheric Thermal Inversion Over the Arabian Sea Using Radiosonde and IASI Data, IEEE](#)
813 [Journal of Selected Topics in Applied Earth Observations and Remote Sensing, 9, 490-495, doi:](#)
814 [10.1109/JSTARS.2015.2506759, 2016.](#)

Comment [S1]: Dwivedi et al.
As per the format

815 Gadgil, S., and Joseph, P. V.: On breaks of the Indian monsoon, *Proc. Indian Acad. Sci.*, 112, 529–
816 558, 2003.

817 Kidder, S. Q., and Haar, T. H.V., Academic press inc., California, U.S.A.: Satellite Meteorology -
818 An Introduction, ISBN 0-12-406430-2,199, 1995.

819 Kripalani, R. H., Kulkarni, S. A., Sabade, S., Revadekar, J. V., Patwardhan, S. K., and Kulkarni, J.
820 R.: Intra-seasonal oscillations during monsoon 2002 and 2003, *Curr. Sci.*, 87, 325– 331, 2004.

821 Kwon, E.H., Sohn, B. J., William, L., and Smith, J. L.: Validating IASI temperature and moisture
822 sounding retrievals over East Asia using radiosonde observations, *J. Atmos. Oceanic Technol.*, 29,
823 1250–1262, doi:10.1175/JTECH-D-11-00078.1, 2012.

824 Kursinski, E. R., Hajj, G. A., Schofield, J. T., Linfield, R. P. and Hardy, K. R.: Observing Earth’s
825 atmosphere with radio occultation measurements using the Global Positioning System, *J. Geophys.*
826 *Res.*, 102, 23,429–23,466, doi:10.1029/97JD01569, 1997.

827 Lambrigtsen, B. H.: Calibration of the AIRS microwave instruments, *IEEE Trans. Geosci. Remote*
828 *Sens.*, 41, 369–378, 2003.

829 Narayanan, M. S., and Rao, B. M.: Detection of monsoon inversion by TIROS-N satellite, *Nature*,
830 294, 546 – 548, 1981.

831 Narayanan, M. S., and Rao, B. M.: Stratification and convection over Arabian Sea during monsoon
832 1979 from satellite data, *Proc. Indian Acad. Sci. (Earth Planet. Sci.)*, 98, 4, 339-352, 1989.

833 Narayanan, M. S., Rao, B.M. , Shah, S., Prasad, V. S., and Bhat, G.S.: Role of atmospheric stability
834 over the Arabian Sea and the unprecedented failure of monsoon 2002, *Curr. Sci. enee*, 86, 7, 938
835 – 947, 2004.

836 Rajeevan, M., and Bhate, J.: A high resolution daily gridded rainfall data set (1971–2005) for
837 mesoscale meteorological studies, *Curr. Sci.*, 96, 558– 562, 2009.

838 Rajeevan, M., Bhate, J., Kale, J. D., and Lal, B.: High resolution daily gridded rainfall data for the
839 Indian region: Analysis of break and active monsoon spells, *Curr. Sci.*, 91, 296– 306, 2006.

840 Ramage, C. S.: The Summer Atmospheric Circulation over the Arabian Sea, *J. Atmos. Sci.*, 23, 144
841 – 150, 1966.

842 Roja Raman, M., Venkat Ratnam, M., Rajeevan, M., Jagannadha Rao, V.V.M., and Vijaya Bhaskara
843 Rao, S.: Intriguing aspects of monsoon low level jet over peninsular India revealed by high-
844 resolution GPS radiosonde observations, *J. Atmos. Sci.*, 68, 1413-1423, [doiDOI:](https://doi.org/10.1175/2011JAS3611.1)
845 10.1175/2011JAS3611.1, 2011.
846 [Sanjeev et al. \(2016\)](#)
847
848 Sathiyamoorthy, V., Mahesh, C., Gopalan, K., Prakash, S., Shukla, B. P. and Mathur, A. K.:
849 Characteristics of low clouds over the Arabian Sea, *J. Geophys. Res.*, 118, 24, 13,489–13,503,
850 2013.
851 Schlüssel, P., Hultberg, T. H., Philipps, P. L., August, T., and Calbet, X.: The operational IASI level
852 2 processor, *Adv. Space Res.*, 36, 982–988, doi:10.1016/j.asr.2005.03.008, 2005.
853 Simmons, A. J., and Hollingsworth A.: Some aspects of the improvement in skill of numerical
854 prediction, *Q. J. R. Meteor. Soc.*, 128, 647–677, 2002.
855 Simmons, A., Uppala, S., and Dee, D.: Update on ERA-Interim, *ECMWF News L.*, 111, 5, 2007.
856 Simon, B., Rahman, S. H., Joshi, P. C. and Desai, P. S.: Shifting of the convective heat source over
857 the Indian Ocean region in relation to performance of monsoon: a satellite perspective, *Inter. J. of*
858 *Rem. Sens.*, 29:2, 387 – 397, doi: 10.1080/01431160701271966, 2007.
859 [Smith, N., Smith Sr., W. L., Weisz, E., and Revercomb, H. E.; Smith, N., William L. Smith Sr., Elisabeth](#)
860 [Weisz, and Henry E. Revercomb;](#) AIRS, IASI, and CrIS Retrieval Records at Climate Scales: An
861 Investigation into the Propagation of Systematic Uncertainty, *Am. Meteorol. Soc.*, 54, 1565 – 1481,
862 [doiDOI:](https://doi.org/10.1175/JAMC-D-14-0299.1) 10.1175/JAMC-D-14-0299.1, 2015.
863 Susskind, J., Barnet, C. D., and Blaisdell, J.M.: Retrieval of atmospheric and surface parameters
864 from AIRS/AMSU/HSB data in the presence of clouds, *IEEE Trans. Geosci. Rem. Sem.*, 41, 390-
865 409, 2003.

Formatted: Font: Times New Roman, No underline, Font color: Auto

Formatted: No underline, Font color: Auto

866 Thomas W. S.: An assessment of Operational TIROS – N Temperature Retrievals over the United
867 States, Monthly Weather Review, [American Meteorological Society](#), 109, 110-119, 1981.

868 Wallace, J. M. and Hobbs, P. V., International Geophysics series: Atmospheric Science - An
869 Introductory Survey, Second Edition, 92, ISBN 13: 978-0-12-732951-2, 391, 2006,.
870 WMO, GARP Publication series no.18, The Monsoon Experiment, 1976.

871
872
873
874
875
876

877 **Figure captions:**

878 **Figure 1.** Typical examples showing MI in T and RH on (a) 27 June 1979 at 0730 GMT at 20°N,
879 60°E measured by radiosonde during MONEX experiment~~obtained from radiosonde from MONEX~~
880 experiment, (b) same as (a) but at 0600 GMT from ERA, (c) 30 July 2009 at 0514 GMT at 22°N,
881 68°E by IASI, (d) 30 July 2009 by ERA-Interim at same location but at 0600 GMT. Note that scale
882 for RH is shown in the top axis of (a) and (b).

883 **Figure 2.** Time series of ΔT for starting and ending of MI from April to October 2009 (black) and
884 2011 (blue). Green vertical lines are showing starting (01 May 2009) and ending (07 October 2009)
885 time for MI.

886 **Figure 3.** Base altitude occurrence of MI during (a) July, (b) August, ΔT (Strength) of MI (c) July,
887 (d) August, and Percentage occurrence of MI days (e) July, (f) August, averaged during 2009-2013
888 observed by IASI- (We are selecting WAS, CAS and EAS from this figure).

889 **Figure 4.** Percentage occurrence of (a) ΔT and (b) q at 700 hPa observed in WAS and EAS during
890 monsoon season of the years 2009-2013 for various ranges of ΔT and q at 700 hPa by IASI. (c) and
891 (d) same as (a) and (b) but obtained from ERA-Interim data.

892 **Figure 5.** Time series of (a) ΔT and (b) q at 700 hPa observed over WAS and EAS grid boxes
893 during the monsoon season of the year 2012 by IASI, (c) and (d) same as (a) and (b) but obtained
894 using ERA – Interim data. 3-point smoothed curves are shown.

895 **Figure 6.** MI observed in (a) ΔT and (b) q at 700 hPa during break spells (30 July – 11 August 2009)
896 of the year 2009 by IASI, (c) and (d) same as (a) and (b) but observed during active spells (14-17
897 July 2009). (e) and (f) and (g) and (h), same as (a) and (b) and (c) and (d) but observed by ERA-
898 Interim, respectively.

899 **Figure 7.** Time variations of (a) ΔT and (b) q at 700 hPa observed over WAS during two contrasting
900 years of 2009 and 2011 by using IASI measurements and ERA-Interim products (e and f).
901 Difference between 2011 and 2009 observed in (c) ΔT and (d) q at 700 hPa for IASI and ERA-

902 ~~Inrerim products (g and h).-(e) to (h) same as (a) to (d) but observed by using ERA Interim data~~
903 ~~products.~~

904 **Figure 8.** Percentage occurrence of MI observed with (a) $\Delta T \leq 2K$ using IASI, AIRS and ERA-
905 Interim data during monsoon seasons of 2009-2013 over WAS and EAS.

906 **Figure 9.** Typical examples showing MI in temperature and RH on (a) 27 June 1979 at 0656 GMT at
907 $20^{\circ}N$, $62^{\circ}E$ obtained from dropsondes from MONEX experiment, (b) N profile (c) Scatter plot of
908 ΔT and ΔN .

909 **Figure 10.** Frequency of ΔN observed in Western AS and Eastern AS during monsoon season of the
910 years 2009-2013 for various ranges of ΔN by COSMIC. Western AS is showing higher
911 valuesmeans inversion is there.

912

913 **Table captions:**

914 **Table 1:** Data details for accuracy/error and availability.

915 **Table 2:** Comparison of aircraft profiles with satellite data.

916 **Table 1:** Data details for accuracy/error and availability.

	IASI	AIRS	COSMIC GPS - RO	ERA-Interim	MONEX 1979 In-situ data
Launch of satellite	MetOp – A launched in October 2006, 8461 spectral Channels	Aqua launched in May 2002, 2378 spectral channels	GPS – RO microsatellite receiver launched in April 2006	---	May – August 1979
Data availability from	August 2008	2003	April 2006	1979	May – August 1979
Data used in the present study	June – September 2009 - 2013	June – September 2009 – 2013	June – September 2009 - 2013	June – September 2009 - 2013	May – August 1979
Accuracy in Temperature	~ 1 K(RMS) at a vertical resolution of 1 Km(Clerbaux et al., 2007; 2009)	~ 1 K at a vertical resolution of 1 Km(Susskind et al., 2003)	Generally ~ 100m in the lower troposphere (not for T)	0.5 – 1.0 K at a vertical resolution of 0.8 – 1.0 km	± 1 °C in 4 vertical levels resolution(WMO report)
Accuracy in Humidity	~10 – 15 % accuracy with a 1 – 2 Km vertical resolution(Clerbaux et al., 2007; 2009)(Schlüssel et al., 2005)	~15 % accuracy with a 2 Km vertical layer resolution(Susskind et al., 2003)	---	~7.0 – 20 % at a vertical resolution of 0.8 – 1.0 km	± 30 % at a vertical resolution of 4 levels.
Accuracy in Refractivity	---	---	400 m to 1.4 km (Kursinski et al., 1997),		
Horizontal resolution	15 Km	25 Km	2000 soundings per day	1.5° x 1.5° (~ 80 km)	500 km
Pressure levels	1100- 0.0161 hPa - 100	1100 – 0.0161 hPa – 100	70% of occultations penetrate below 1 km (Anthes et al., 2008)	1013 – 1 hPa 37	1000 – 294 Different -2
Local equator crossing time	0930 LT descending node	1330 LT ascending node	-----	----	---
Swath	2200 km	1650 Km	-----		

917

918

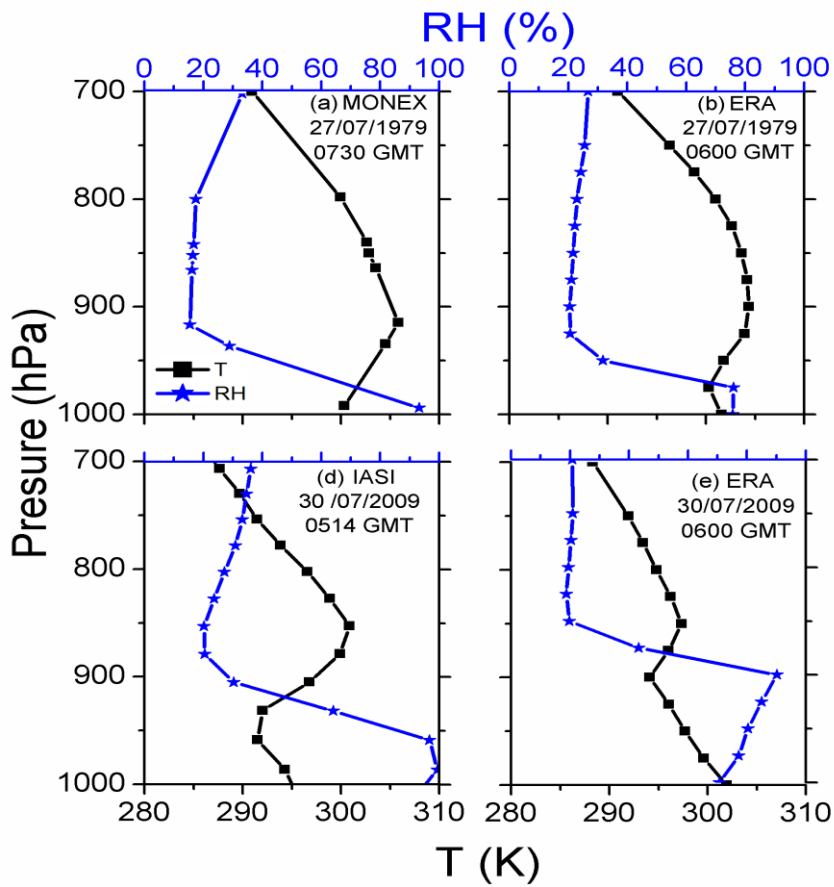
919 **Table 2:** Comparison of aircraft profiles with satellite data.

	Aircraft profiles	Near simultaneous satellite data	
		$\Delta T \leq 2^{\circ}\text{C}$	$\Delta T \geq 3^{\circ}\text{C}$
No. Of profiles with well – marked inversion below 850 mbar	30	23	7 (for four of them $\Delta T = 3^{\circ}\text{C}$)
No. Of profiles without well – marked inversion	129	0	129

920 (Regenerated from Narayanan et al., 1981)

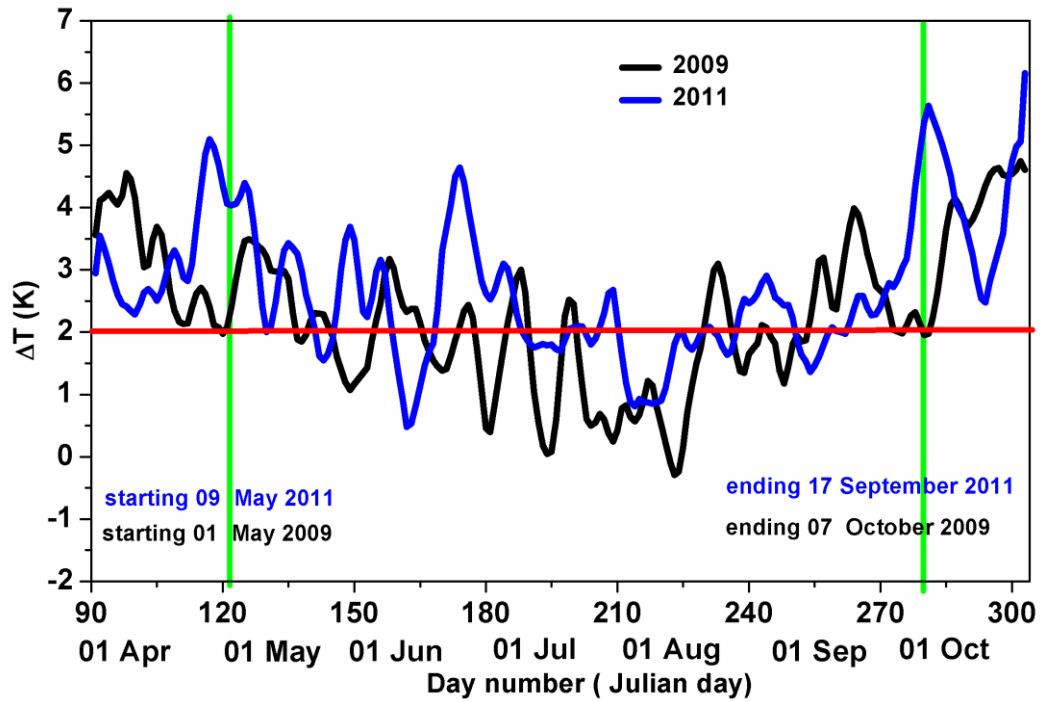
921

922 **Figures:**



923

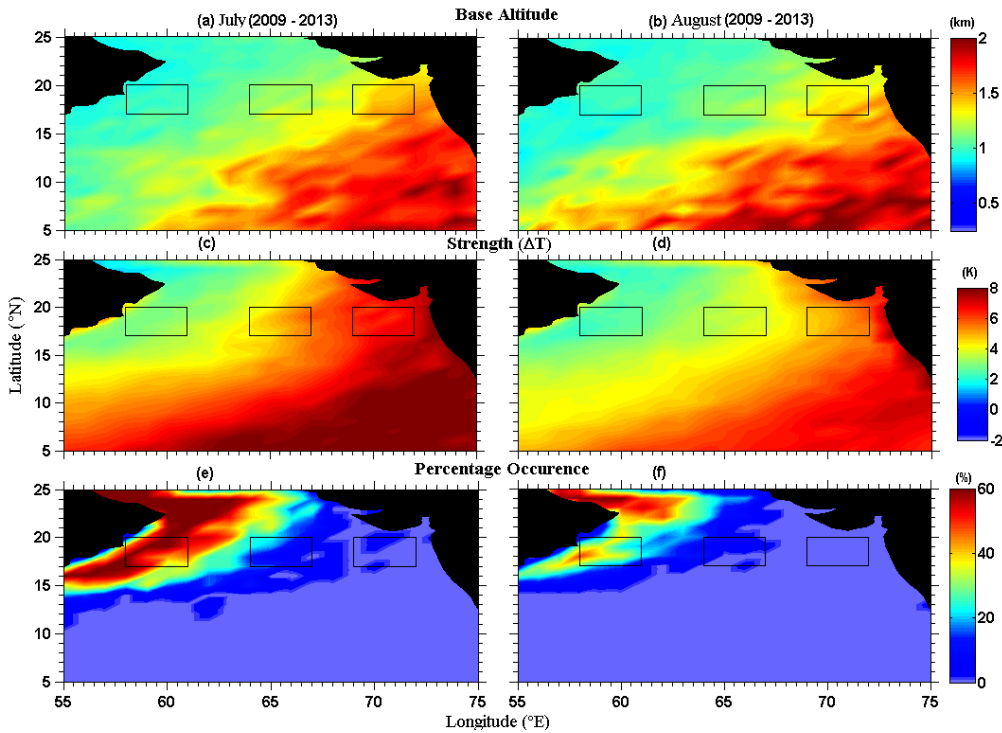
924 **Figure 1.** Typical examples showing MI in T and RH on (a) 27 June 1979 at 0730 GMT at 20°N,
925 60°E measured by radiosonde during MONEX experiment~~obtained from radiosonde from MONEX~~
926 experiment, (b) same as (a) but at 0600 GMT from ERA, (c) 30 July 2009 at 0514 GMT at 22°N,
927 68°E by IASI, (d) 30 July 2009 by ERA-Interim at same location but at 0600 GMT. Note that scale
928 for RH is shown in the top axis of (a) and (b).



929

930 **Figure 2.** Time series of ΔT for starting and ending of MI from April to October 2009 (black) and
 931 2011 (blue). Green vertical lines are showing starting (01 May 2009) and ending (07 October 2009)
 932 time for MI.

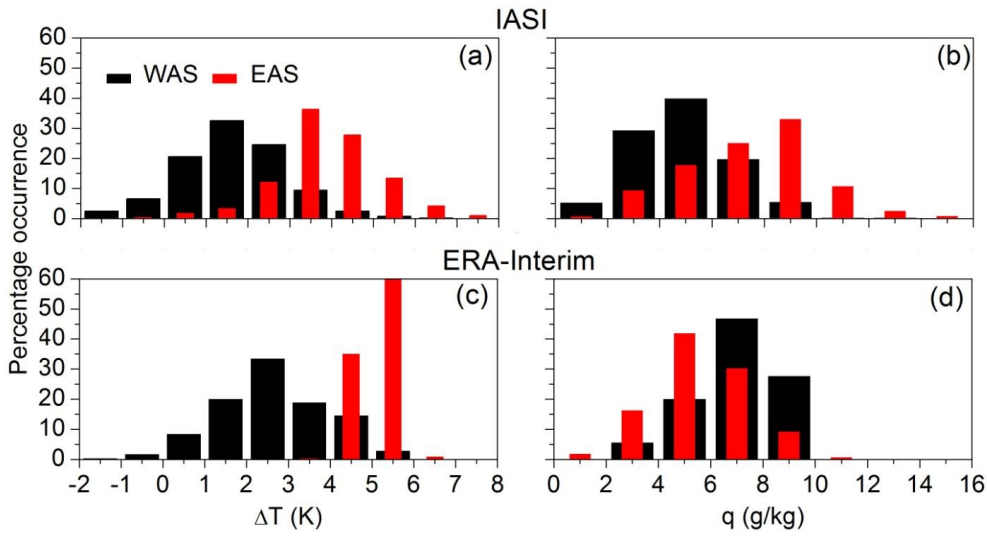
933



934 **Figure 3.** Base altitude occurrence of MI during (a) July, (b) August, ΔT (Strength) of MI (c) July,
 935 (d) August, and Percentage occurrence of MI days (e) July, (f) August, averaged during 2009-2013
 936 observed by IASI- (We are selecting WAS, CAS and EAS from this figure).
 937

938
 939
 940
 941
 942
 943
 944
 945
 946
 947

948



949

950 **Figure 4.** Percentage occurrence of (a) ΔT and (b) q at 700 hPa observed in WAS and EAS during
951 monsoon season of the years 2009-2013 for various ranges of ΔT and q at 700 hPa by IASI. (c) and
952 (d) same as (a) and (b) but obtained from ERA-Interim data.

953

954

955

956

957

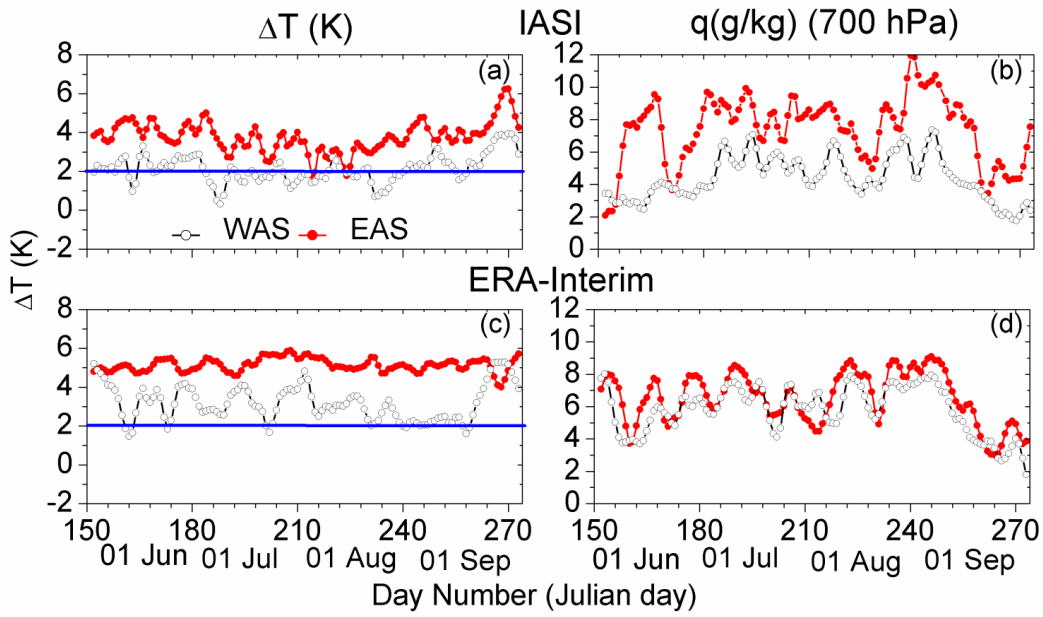
958

959

960

961

962



963

964 **Figure 5.** Time series of (a) ΔT and (b) q at 700 hPa observed over WAS and EAS grid boxes
 965 during the monsoon season of the year 2012 by IASI, (c) and (d) same as (a) and (b) but obtained
 966 using ERA – Interim data. 3-point smoothed curves are shown.

967

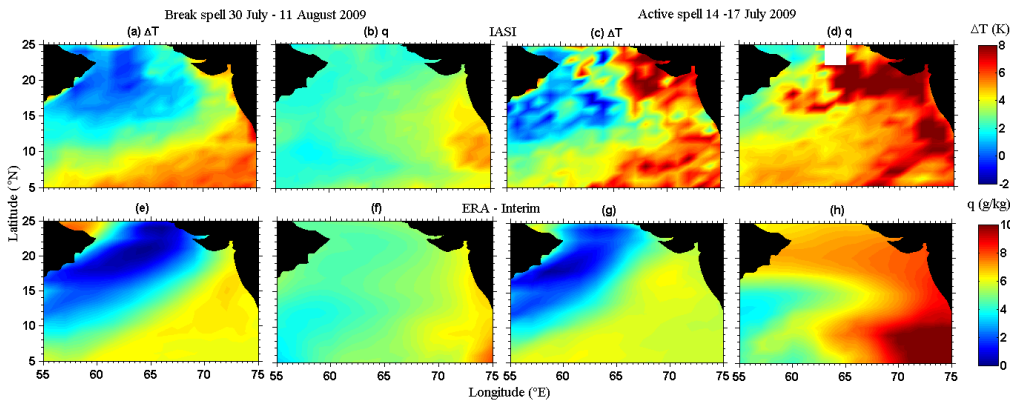
968

969

970

971

972



973 **Figure 6.** MI observed in (a) ΔT and (b) q at 700 hPa during break spells (30 July – 11 August
 974 2009) of the year 2009 by IASI, (c) and (d) same as (a) and (b) but observed during active spells
 975 14-17 July 2009). (e) and (f) and (g) and (h), same as (a) and (b) and (c) and (d) but observed by
 976 ERA-Interim, respectively.
 977

978

979

980

981

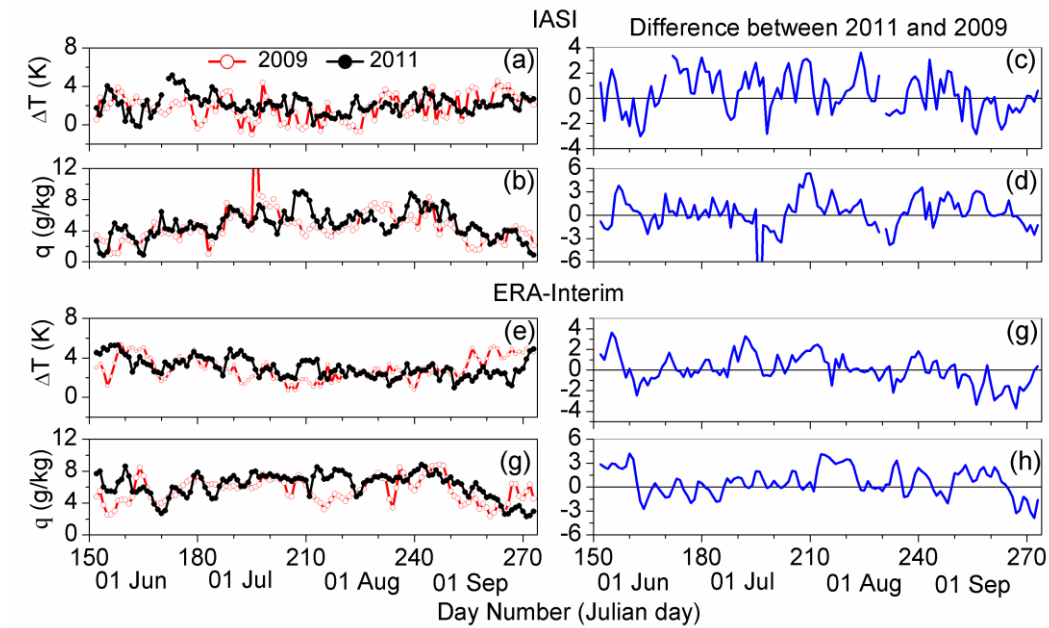
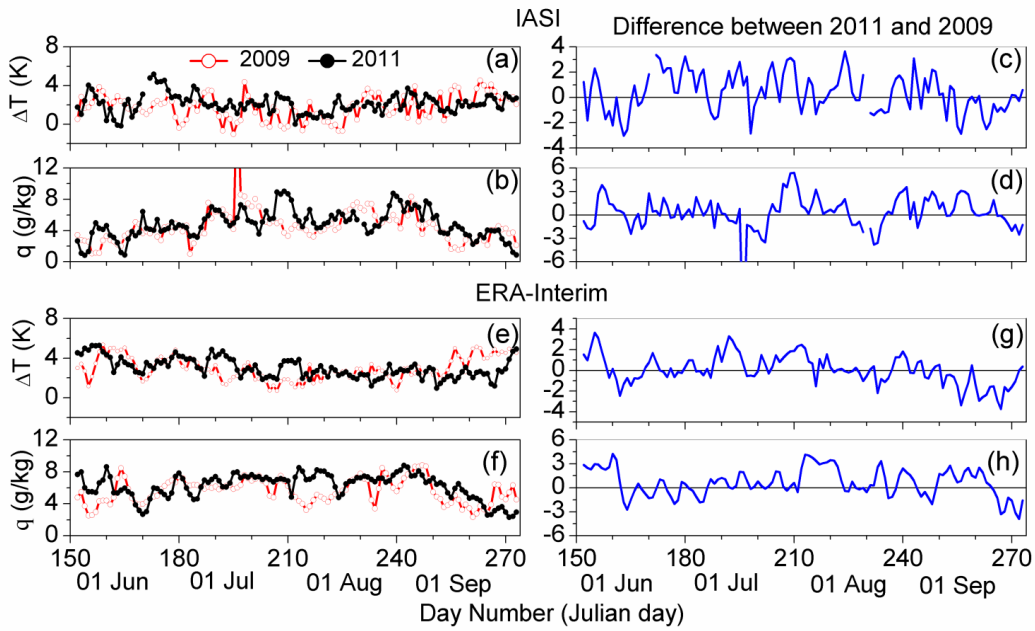
982

983

984

985

986



988 **Figure 7.** Time variations of (a) ΔT and (b) q at 700 hPa observed over WAS during two
 989 contrasting years of 2009 and 2011 by using IASI measurements. Difference between 2011 and
 990 2009 observed in (c) ΔT and (d) q at 700 hPa. (e) to (h) same as (a) to (d) but observed by using
 991 ERA-Interim data.
 992

993 **Figure 7. Time variations of (a) ΔT and (b) q at 700 hPa observed over WAS during two contrasting**
994 **years of 2009 and 2011 by using IASI measurements and ERA-Interim products (e and f).**
995 **Difference between 2011 and 2009 observed in (c) ΔT and (d) q at 700 hPa for IASI and ERA-**
996 **Interim products (g and h).**

997

998

999

1000

1001

1002

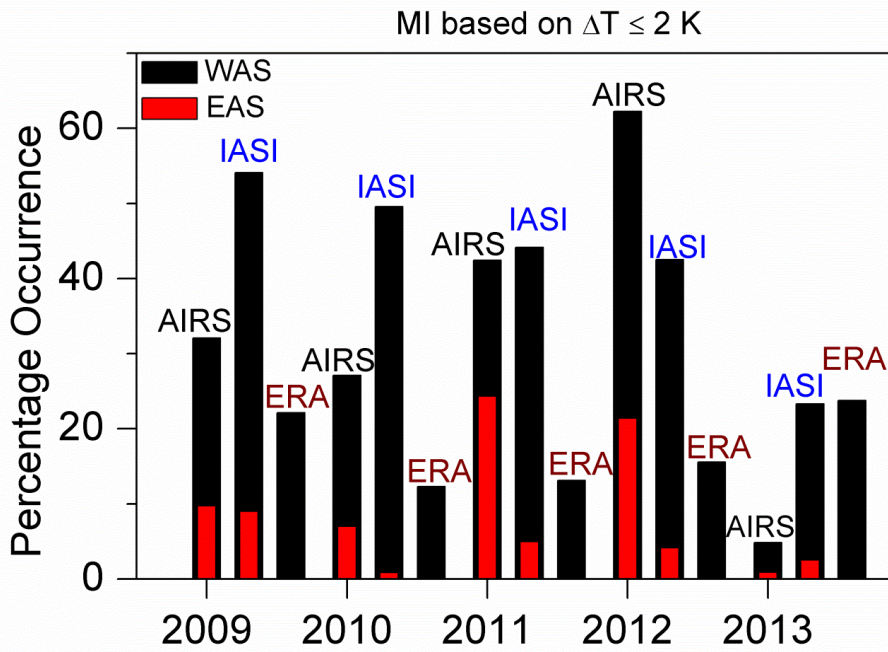
1003

1004

1005

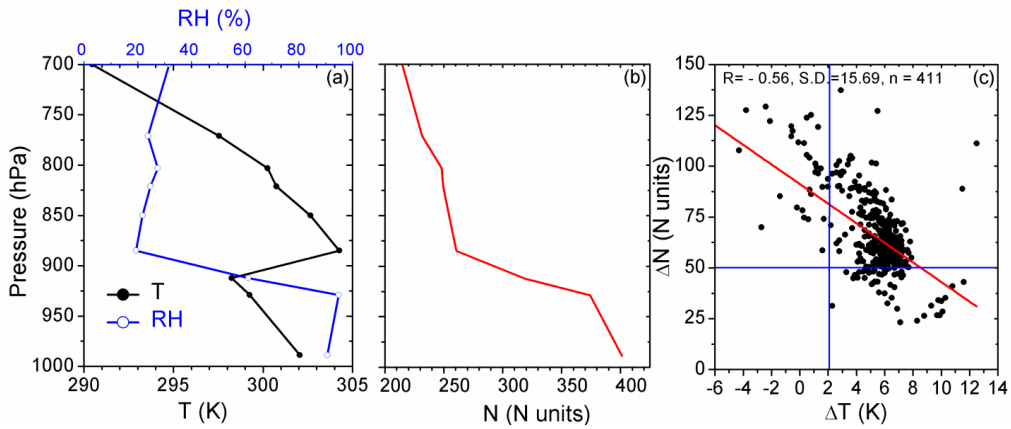
1006

1007



1008
 1009 **Figure 8.** Percentage occurrence of MI observed with (a) $\Delta T \leq 2\text{K}$ using IASI, AIRS and ERA-
 1010 Interim data during monsoon seasons of 2009-2013 over WAS and EAS.

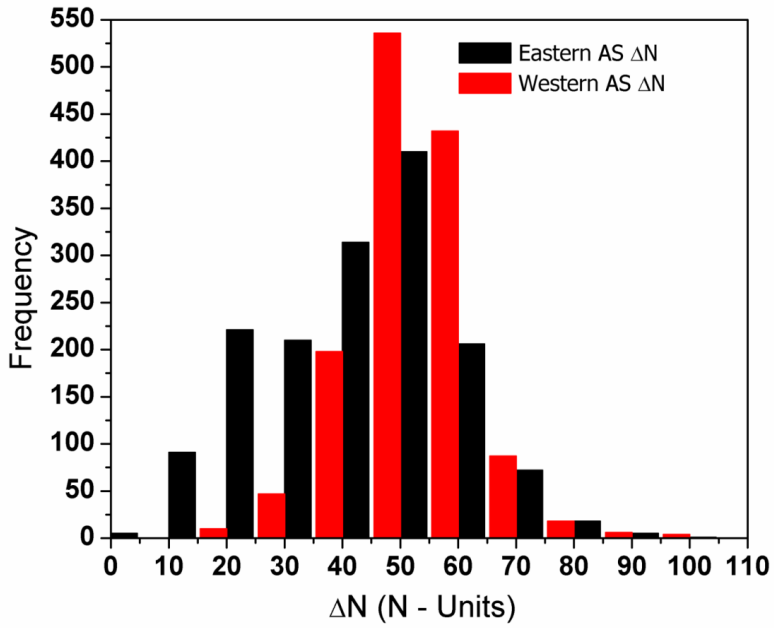
1011
 1012
 1013
 1014



1015
 1016 **Figure 9.** Typical examples showing MI in temperature and RH on (a) 27 June 1979 at 0656 GMT
 1017 at 20°N, 62°E obtained from dropsondes from MONEX experiment, (b) N profile (c) Scatter plot of
 1018 ΔT and ΔN .

1019
 1020
 1021
 1022
 1023
 1024
 1025
 1026
 1027
 1028
 1029
 1030
 1031
 1032
 1033

1034
1035
1036
1037
1038



1039
1040
1041
1042
1043
1044

Figure 10. Frequency of ΔN observed in Western AS and Eastern AS during monsoon season of the years 2009-2013 for various ranges of ΔN by COSMIC. Western AS is showing higher values means inversion is there.